IMPROVED DETECTION OF A TARGET ON A RANDOM ROUGH SURFACE USING ANGULAR CORRELATION FUNCTION

Sermsak Jaruwatanadilok[1], Sumit Roy[2], and Yasuo Kuga[2]

1 Jet Propulsion Laboratory, California Institution of Technology, Pasadena, CA, USA
2 Department of Electrical Engineering, University of Washington, Seattle, WA, USA

1. INTRODUCTION

Detection of a target in cluttered environment based on electromagnetic wave scattering has been considered for many years [1-3]. In this work, we consider detection of a target situated on top of a random rough surface, whereby the scatter component from the surface is considered to be background clutter. Detector design is traditionally based on the ***difference*** in the characteristics of the returned signal from background clutter alone vis-à-vis target+clutter, and usually only exploits the differences in the observed wave ***intensity*** (or equivalently, radar cross section or RCS) [4],[5]. Our primary contribution is the analysis of detection probability when using the angular correlation function (ACF) for enhanced detection which correlates the scattered signal at two different angles. The ACF has been used in subsurface detection [6],[7], but there is no analysis of the improvement in detection in terms of probability of detection and false alarm. In our previous work, we exploited the strong correlation from rough surface scattering for sea-ice [8] and snow thickness determination [9]. However, for target detection on random rough surface, the effect from rough surface scattering is to be minimized. The scattered signal from the background as a function of elevation angle exhibits strong peaks at certain combination of frequencies and incident and observed angles. Hence, by careful choice of transmitting frequencies and incident and observed angles, we should be able to reduce the effects of rough surface scattering. Here, we derive the statistical properties of the ACF of a scattered wave from a random rough surface and its relationship to the physical parameters of the rough surface and observation system geometry. Then we analyze the probability of detection versus probability of false alarm using ACF and RCS which shows that the receiver operating characteristics (ROC) of the detector using ACF is conclusively superior to that using RCS.

2. FORMULATION AND NUMERICAL SIMULATIONS USING FDTD

In our geometry (Fig. 1), the medium 1 is free space ($\varepsilon_1 = \varepsilon_o$; $\mu_1 = \mu_o$) while medium 2 is a lossy dielectric. We define the intrinsic propagation constant of medium 2 by $\alpha_2 + j\beta_2 = j2\pi f\sqrt{\varepsilon_{r2}}/c$ where ε_{r2} is the complex relative dielectric constant of medium 2. α_2 represents a loss constant while β_2 represents a phase constant. The wave number is given by $k_1 = 2\pi f/c$, f is the frequency of the wave, c is the speed of light and $\beta_1 = k_1$. The far-field scattered wave is given by [10]

$$\psi_{obs}^{[1]}(K_{obs}, K_{inc}) = \frac{k_1 \cos\theta_{obs}^{[1]}}{\left(2\pi k_1 R^{[1]}\right)^{1/2}} \exp\left(-jk_1 R^{[1]} + j\frac{\pi}{4}\right) S(K_{obs}^{[1]}, K_{inc}^{(1)})\psi_{inc}^{(1)} \quad (1)$$

where $R^{[1]}$ is the distance from the illuminated area to the observation point $S(K_{obs}^{[1]}, K_{inc}^{(1)}) = \gamma(K_{obs}^{[1]}, K_{inc}^{(1)})H(K_{obs}^{[1]}, K_{inc}^{(1)})$,

$$\gamma(K_{obs}^{[1]}, K_{inc}^{(1)}) = \frac{1}{2\pi}\frac{jK_{z2}^{(1)}A/\varepsilon_r + B}{jK_{z2}^{(1)}/\varepsilon_r + jK_{inc\_z}^{(1)}},\ A = \left(jK_{inc\_z}^{(1)} - jK_{z1}^{(1)}\Gamma - jK_{z2}^{(1)}T\right),\ B = \left(-(K_{inc}^{(1)}K_{obs}^{[1]} - k_1^2)(1+\Gamma) + \frac{1}{\varepsilon_r}(K_{inc}^{(1)}K_{obs}^{[1]} - k_2^2)T\right)$$

$$\varepsilon_r = \frac{\varepsilon_2}{\varepsilon_1},\ K_{inc}^{(1)} = \beta_1 \sin\theta_{inc}^{(1)},\ K_{inc\_z}^{(1)} = \beta_1\cos\theta_{inc}^{(1)},\ K_{z1}^{(1)} = \sqrt{k_1^2 - \left(K_{inc}^{(1)}\right)^2},\ K_{z2}^{(1)} = \sqrt{k_2^2 - \left(K_{inc}^{(1)}\right)^2},\ K_{obs}^{[1]} = \beta_1\sin\theta_{obs}^{[1]},\ K_{obs}^{[2]} = \beta_1\sin\theta_{obs}^{[2]}$$

Γ is the reflection coefficient, and T the transmission coefficient. For TE waves $\Gamma = \dfrac{\sqrt{\varepsilon_1}\cos\theta_{inc}^{(1)} - \sqrt{\varepsilon_2}\cos\theta_{inc2}^{(1)}}{\sqrt{\varepsilon_1}\cos\theta_{inc}^{(1)} + \sqrt{\varepsilon_2}\cos\theta_{inc2}^{(1)}}$,

$T = \dfrac{2\sqrt{\varepsilon_1}\cos\theta_{inc}^{(1)}}{\sqrt{\varepsilon_1}\cos\theta_{inc}^{(1)} + \sqrt{\varepsilon_2}\cos\theta_{inc2}^{(1)}}$, and for TM waves $\Gamma = \dfrac{\sqrt{\varepsilon_2}\cos\theta_{inc}^{(1)} - \sqrt{\varepsilon_1}\cos\theta_{inc2}^{(1)}}{\sqrt{\varepsilon_2}\cos\theta_{inc}^{(1)} + \sqrt{\varepsilon_1}\cos\theta_{inc2}^{(1)}}$, $T = \dfrac{2\sqrt{\varepsilon_2}\cos\theta_{inc}^{(1)}}{\sqrt{\varepsilon_2}\cos\theta_{inc}^{(1)} + \sqrt{\varepsilon_1}\cos\theta_{inc2}^{(1)}}$. The relationship between $\theta_{inc}^{(1)}$ and $\theta_{inc2}^{(1)}$ can be found using Snell's law: $\sqrt{\varepsilon_1}\sin\theta_{inc}^{(1)} = \sqrt{\varepsilon_2}\sin\theta_{inc2}^{(1)}$. Define

$H(K_{obs}^{[1]}, K_{inc}^{(1)}) = \int h(x)\exp\left(-j(K_{obs}^{[1]} - K_{inc}^{(1)})x\right)dx$ where $h(x)$ is the vertical displacement or height relative to a baseline of the random surface. The angular correlation function of the observed complex amplitude is now given by

$$\begin{aligned}\left\langle \psi_{obs}^{[1]}(K_{obs}^{[1]}, K_{inc}^{(1)})\psi_{obs}^{[2]*}(K_{obs}^{[2]}, K_{inc}^{(1)})\right\rangle = \frac{k_1^2 \cos\theta_{obs}^{[1]} \cos\theta_{obs}^{[2]}}{2\pi k_1 \left(R^{[1]}R^{[2]}\right)^{1/2}} \exp\left(-j(k_1 R^{[1]} - k_1 R^{[2]})\right)\gamma(K_{obs}^{[1]}, K_{inc}^{(1)}) \\ \gamma^*(K_{obs}^{[2]}, K_{inc}^{(1)})\left\langle H(K_{obs}^{[1]}, K_{inc}^{(1)})H^*(K_{obs}^{[2]}, K_{inc}^{(1)})\right\rangle \psi_{inc}^{(1)}\psi_{inc}^{(1)*}\end{aligned} \tag{2}$$

where $\left\langle H(K_{obs}^{[1]}, K_{inc}^{(1)})H^*(K_{obs}^{[2]}, K_{inc}^{(1)})\right\rangle = \iint \left\langle h(x)h(x')\right\rangle \exp\left(-j\left(K_{obs}^{[1]} - K_{inc}^{(1)}\right)x\right)\exp\left(+j\left(K_{obs}^{[2]} - K_{inc}^{(1)}\right)x'\right)dx\,dx'$.

For a Gaussian random surface with tapered plane wave with illumination $W(x) = \exp\left(-x^2/2L_{eq}^2\right)$ and Gaussian auto-correlation as above. We obtained

$$\left\langle H(K_{obs}^{[1]} - K_{inc}^{(1)})H^*(K_{obs}^{[2]} - K_{inc}^{(1)})\right\rangle = \sigma_h^2 \pi L_{eq} l \exp\left(-\frac{A_c^2 l^2}{4}\right)\exp\left(-\frac{A_d^2 L_{eq}^2}{4}\right) \tag{3}$$

where $A_c = (A+B)/2$, $A_d = A - B$, $A = K_{obs}^{[1]} - K_{inc}^{(1)}$, $B = K_{obs}^{[2]} - K_{inc}^{(1)}$. l =correlation length, σ_h =rms height, and L_{eq} = illumination length. We employ the RCS definition [11] of $\mathrm{RCS} = \lim_{R\to\infty} 2\pi R\left|\psi_{obs}\right|^2 / \left|\psi_{inc}\right|^2$. Note from (1), ψ_{obs} in the far-field is a function of $1/\sqrt{R}$ and the RCS thus does not depend on R. For our two-dimensional geometry, RCS is the scattering width or the radar cross section per unit length (and has units of length) [12]. For a fair comparison, we employ the ACF definition $\mathrm{ACF} = \lim_{R\to\infty} 2\pi R\left|\left\langle \psi_{obs}^{[1]}(K_{obs}^{[1]}, K_{inc}^{(1)})\psi_{obs}^{[2]*}(K_{obs}^{[2]}, K_{inc}^{(1)})\right\rangle\right| / \left|\psi_{inc}\right|^2$ which also has units of length.

We investigate the behavior of the angular correlation function and the radar cross section for the scattered waves in two cases where (1) a target is present on a random rough surface and (2) no target is present (rough surface only). Previously, we derived the analytical solution for ACF for rough surface scattering. However, when a target is present, the analytical solution for a scattered wave is not tractable because of the complex interaction between the target and the random rough surface. Therefore, we employ numerical simulations using the two-dimensional finite-difference time-domain (FDTD) method. The geometry of the simulations is illustrated in Fig. 1. Wave scattering is simulated and the observed wave is calculated in the situation where the perfect electric conductor (PEC) target is present and when there is no target. The rough surface interface has a Gaussian correlation function with the rms height of 2.4 cm and correlation length of 12 cm. The PEC target has a radius of 10 cm, the center frequency of the incident wave is 1.5 GHz, the ground dielectric constant is $3.7 - j0.1$. The surface length of the simulation is 200 wavelengths. The incident wave is a tapered plane wave with an incident angle of 20^o. The grid resolution in the simulation is 50 points per wavelength. PML is used to absorb out-going wave and prevent erroneous scattering.

3. PROBABILISTIC MODEL OF RCS AND ACF

The p.d.f. for the RCS of the Gaussian random surface was derived by [14] and is in the form of an exponential distribution

$$f_{\mathrm{U}}(u) = \frac{1}{2\sigma_R^2 \left|K_1\right|^2}\exp\left(-\frac{u}{2\sigma_R^2\left|K_1\right|^2}\right); \quad u \ge 0 \tag{4}$$

where the parameter u relates to the RCS by $u = \mathrm{RCS}\,\lambda/L_{eq}$,

$\left|K_1\right| = j2k\cos\theta_{inc}^{(1)}\cos\theta_{obs}^{[1]}\dfrac{\cos\theta_{obs}^{[1]} - \sqrt{n_2^2 - \sin^2\theta_{obs}^{[1]}}}{\cos\theta_{obs}^{[1]} + \sqrt{n_2^2 - \sin^2\theta_{obs}^{[1]}}}$, $\sigma_R^2 = \dfrac{1}{2}\left[\hat{S}_{aa}(\xi) + \dfrac{\sin(\xi L_{eq})}{\xi L_{eq}}\hat{S}_{aa}(0)\right]$, $\xi = k_1\left(\sin\theta_{inc}^{(1)} - \sin\theta_{obs}^{[1]}\right)$,

and $\hat{S}_{aa}$ is the power spectrum of the surface. If the autocorrelation function of the random surface is Gaussian as before, we get $\hat{S}_{aa}(\xi) = \dfrac{\sigma_h^2 l}{2\sqrt{\pi}}\exp\left(-\dfrac{\xi^2 l^2}{4}\right)$ where l =correlation length, σ_h =rms height, and L_{eq} = illumination length.

Consider the p.d.f. of the ACF, using the definition of ACF, we get

$$\mathrm{ACF} = k_1\cos\theta_{obs}^{[1]}\cos\theta_{obs}^{[2]}\left|\gamma_1(K_{obs}^{[1]}, K_{inc}^{(1)})H(K_{obs}^{[1]}, K_{inc}^{(1)})\right|\left|\gamma_2(K_{obs}^{[2]}, K_{inc}^{(1)})H(K_{obs}^{[2]}, K_{inc}^{(1)})\right| = k_1\cos\theta_{obs}^{[1]}\cos\theta_{obs}^{[2]}\left|F_1\right|\left|F_2\right| \tag{5}$$

Note that function $H(K_{obs}^{[1]}, K_{inc}^{(1)})$ is a random function that is the Fourier transform of the random height $h(x)$. The functions $F_1 = \gamma_1(K_{obs}^{[1]}, K_{inc}^{(1)})H(K_{obs}^{[1]}, K_{inc}^{(1)})$ and $F_2 = \gamma_2(K_{obs}^{[2]}, K_{inc}^{(1)})H(K_{obs}^{[2]}, K_{inc}^{(1)})$ are, in general, complex. If the rough surface height has Gaussian characteristics, the real and imaginary parts of these functions are also Gaussian distributed since γ_1 and γ_1 are both complex constants [12]. By transforming to polar coordinates, the real and imaginary parts are converted to magnitude and phase. With the large illumination area ($L_{eq} \to \infty$), we can assume that the magnitude and phase of functions F's are independent [13]. Thus, we find the p.d.f of the magnitude of the function F_1 in the form of Rayleigh distribution as [13]. The p.d.f of ACF is therefore the p.d.f of multiplication of two Rayleigh-distributed random variables with two different parameters and a purely real number scaling. With a large illumination area ($L_{eq} \to \infty$), we can assume that F_1 and F_2 are independent, the distribution of the product of two independent Rayleigh random variables. We obtain the p.d.f of $V = |F_1||F_2|$ as the double-Rayleigh distribution [14],[15], i.e.,

$$f_V(v) = \frac{v}{\sigma_{R1}^2 |\gamma_1|^2 \sigma_{R2}^2 |\gamma_2|^2} K_o\left(\frac{v}{\sigma_{R1}|\gamma_1|\sigma_{R2}|\gamma_2|}\right) \tag{6}$$

where K_o is the modified Bessel function of the second kind and zeroth order. $\sigma_{R1}^2 = \frac{1}{2}\left[\hat{S}_{aa}(\xi_1) + \frac{\sin(\xi_1 L_{eq})}{\xi_1 L_{eq}}\hat{S}_{aa}(0)\right]$, $\xi_1 = k_1\left(\sin\theta_{inc}^{(1)} - \sin\theta_{obs}^{[1]}\right)$, and the expression of $\hat{S}_{aa}$ is given previous for RCS case. From Eq. (5), the parameter V relates to the ACF by $V = \frac{\text{ACF}}{k_1 \cos\theta_{obs}^{[1]} \cos\theta_{obs}^{[2]}}$. The numerical simulations using FDTD are compared to the analytical solution given in Fig.2. In this particular example, the RCS is calculated where the incident and observation angles equal -20^o. The ACF is calculated in the case where the incident wave is -20^o and the observed waves are at -20^o (backscattering) and at -10^o.

4. TARGET DETECTION PERFORMANCE

In the previous section, we analytically determined the p.d.f of ACF and RCS for a scattered wave from a random rough surface which can be used to obtain the probability of false alarm. The determination of the probability of detection requires the p.d.f of the scattered wave when a target is present. However, the complex interaction between the target and the random rough surface precludes any analytical solution for the p.d.f for either the RCS and the ACF, and we resort to FDTD computations to numerically estimate the p.d.f . FDTD calculations of 500 ensembles were used to produce histograms of the RCS magnitude and ACF magnitude. we computed the probability of detection versus probability of false alarm for both the RCS and ACF methods by varying the detection threshold resulting in the receiving operation curve (ROC) shown in Fig. 3. This shows that the ACF method exhibit better performance over RCS in term of probability of detection versus false alarm.

5. ACKNOWLEDGEMENTS

The first author's contribution was performed at the Jet Propulsion Laboratory, California Institute of Technology, under contract with the National Aeronautics and Space Administration. This work is partially supported by the United States Department of Homeland Security through the National Center for Border Security and Immigration (BSI) under grant number 2008-ST-061-BS0002.

6. REFERENCES

[1] D. C. Schleher, "Radar detection in Weibull clutter," *IEEE Transactions on Aerospace and Electronic Systems*, vol. AES-12, no. 6, pp. 736-743, 1976.

[2] M. Hurtado and A. Nehorai, "Polarimetric detection of targets in heavy inhomogeneous clutter," IEEE *Transactions on Signal Processing*, vol. 56, no. 4, pp. 1349-1361, 2008.

[3] B. R. Mahafza, *Radar Systems Analysis and Design Using Matlab*, Boca Raton, FL: Capman & Hall/CRC, 2000.

[4] D. K. Barton, *Radar System Analysis and Modeling*, Boston: Artech House, 2005.

[5] N. A. Goodman, "Optimum and decentralized detection for multistatic airborne radar," *IEEE Transactions on Aerospace and Electronic Systems*, vol. 43, no. 2, pp. 806-813, 2007.

[6] T. K.Chan, Y. Kuga, and A. Ishimaru, "Subsurface detection of a buried object using angular correlation function measurement," *Waves in Random Media*, vol. 7, pp. 457-65, 1997.

[7] S. E. Shih, K. H, Ding, Y. Zhang, and J. A. Kong, "Subsurface detection based on enhanced SAR signatures using angular correlation function," *IGARSS*, Seattle, WA, USA, 1998.

[8] Z. A. Hussein, B. Holt, K. C. McDonald, R. Jordan, J. Huang, Y. Kuga, A. Ishimaru, S. Jaruwatanadilok, S. Gogineni., and T. Akins "High resolution VHF interferometer SAR sensor and technique for sea ice thickness measurement," *IGARSS*, Denver, CO, 2006.

[9] S. Jaruwatanadilok, A. Ishimaru, and Y. Kuga, "Snow thickness estimation using correlation function," *IGARSS*, Anchorage, AK, USA, 2006.

[10] L. Tsang, J. A. Kong, *Scattering of Electromagnetic Waves: Advanced Topics*, New York: John Wiley & Sons, 2001.

[11] C. T. C. Le, Y. Kuga, and A. Ishimaru, "Angular correlation function based on the second-order Kirchhoff approximation and comparison with experiment," *Journal of the Optical Society of America A*, vol. 13, no. 5, pp.1057-67, 1996.

[12] C. A. Balanis, *Advanced Engineering Electromagnetics*, New York: John Wiley & Sons, 1989.

[13] R. Dusseaux and R. de Oliveira, "Effect of the illumination length on the statistical distribution of the field scattered from one-dimensional random rough surfaces: analytical formulae derived from the small perturbation method," *Wave in Random and Complex Media*, vol. 17, no. 3, pp. 305-320, 2007.

[14] J. Salo, H. M. El-Sallabi, and P. Vainikainen, "The distribution of the product of independent Rayleigh random variables," *IEEE Transactions on Antennas and Propagation*, vol. 54, no. 2, pp. 639-643, 2006.

[15] V. Erceg, S. J. Fortue, J. Ling, A. J. Rustako, and R. A. Valenzula, "Comparisons of a computer-based propagation prediction tool with experimental data collected in urban microcellular environments," *IEEE Journal on Selected Areas in Communications*, vol. 15, no.4, pp. 677-684, 1997.

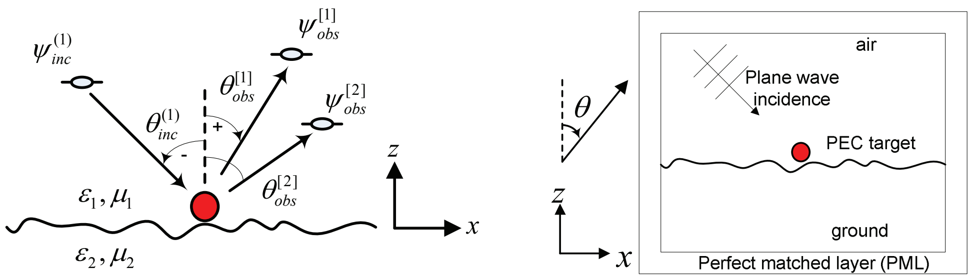

Fig. 1. Left: Geometry of the circular target detection problem. Right: Geometry of FDTD simulations.

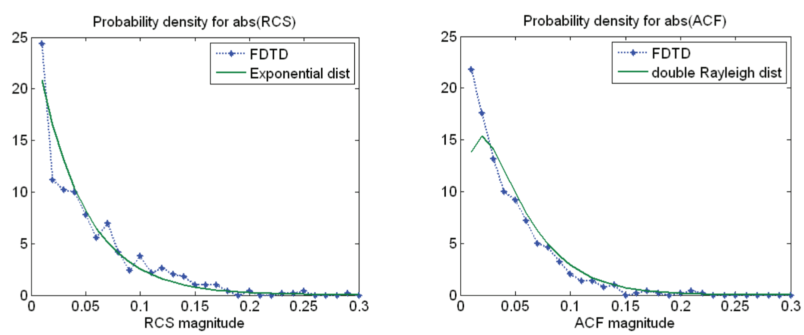

Fig. 2. The p.d.f of magnitude of RCS and ACF comparison between an analytical model and FDTD simulations. Left: P.d.f of RCS comparison between Eq. (4) and FDTD. Right: P.d.f of ACF comparison between Eq. (6) and FDTD.

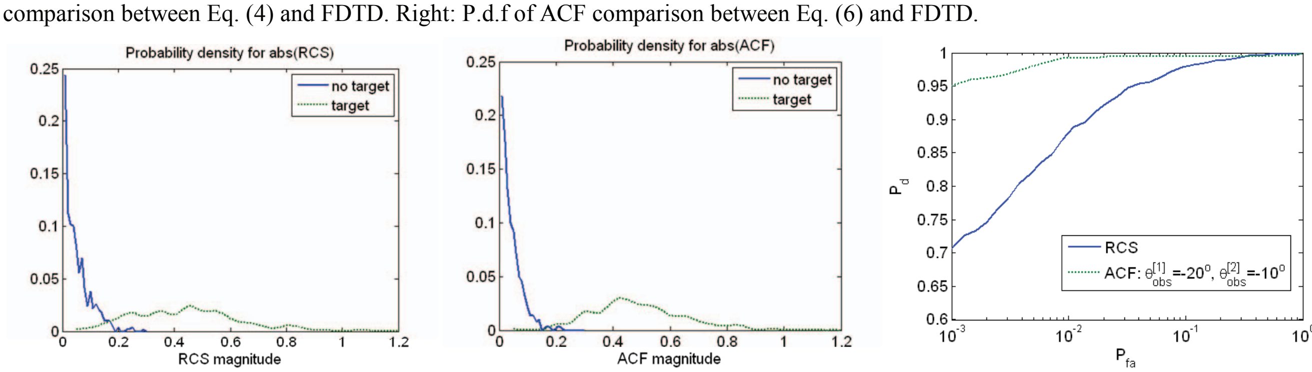

Fig. 3. Probability distribution of RCS and ACF. In this comparison, the incident wave is -20^o. (a) P.d.f of RCS is calculated from the backscattering wave with $\theta_{obs}^{[1]} = -20$, (b) P.d.f. of ACF is calculated from correlation of the observed wave 1 at backscattering direction $\theta_{obs}^{[1]} = -20$ with the observed wave 2 at $\theta_{obs}^{[2]} = -10$, and (c) ROC result.